

Context Aware 3D UNet for Brain Tumor Segmentation

Parvez Ahmad¹[0000-0003-1409-3175], Saqib Qamar²[0000-0002-5980-5976], Linlin Shen², and Adnan Saeed³[0000-0002-0784-5861]

- ¹ National Engineering Research Center for Big Data Technology and System, Services Computing Technology and System Lab, Cluster and Grid Computing Lab, School of Computer Science and Technology, Huazhong University of Science and Technology, 430074, Wuhan, China
parvezamu@hust.edu.cn
- ² Computer Vision Institute, School of Computer Science and Software Engineering, Shenzhen University
sqbqamar@szu.edu.cn, llshen@szu.edu.cn
- ³ School of Hydropower and Information Technology, Huazhong University of Science and Technology, 430074, Wuhan, China
adnansaeed@hust.edu.cn

Abstract. Deep convolutional neural network (CNN) achieves remarkable performance for medical image analysis. UNet is the primary source in the performance of 3D CNN architectures for medical imaging tasks, including brain tumor segmentation. The skip connection in the UNet architecture concatenates features from both encoder and decoder paths to extract multi-contextual information from image data. The multi-scaled features play an essential role in brain tumor segmentation. However, the limited use of features can degrade the performance of the UNet approach for segmentation. In this paper, we propose a modified UNet architecture for brain tumor segmentation. In the proposed architecture, we used densely connected blocks in both encoder and decoder paths to extract multi-contextual information from the concept of feature reusability. The proposed residual inception blocks (RIB) are used to extract local and global information by merging features of different kernel sizes. We validate the proposed architecture on the multimodal brain tumor segmentation challenges (BRATS) 2020 testing dataset. The dice (DSC) scores of the whole tumor (WT), tumor core (TC), and enhancement tumor (ET) are 89.12%, 84.74%, and 79.12%, respectively. Our proposed work is in the top ten methods based on the dice scores of the testing dataset.

Keywords: CNN · UNet · Contextual information · Dense connections · Residual inception blocks · Brain tumor segmentation.

1 Introduction

Brain tumor is the growth of irregular cells in the central nervous system that affect the working of human brains. According to the World Health Organization (WHO), only cancer shares 1 million deaths in 2019. Among them, high-grade glioblastoma(HGG) and low-grade glioblastoma(LGG) are very common. Early diagnosis and accurate brain tumor segmentation can enhance the survival rate of affected patients. Deep CNNs have achieved remarkable performances for brain tumor segmentation [6], [13], [8], [16], [23]. In the diagnosis and treatment planning of glioblastomas, the brain tumor segmentation is required to acquire the actual information from MRI modalities. A 3D UNet is a popular CNN architecture for automatic brain tumor segmentation [9], [14], [22]. The multi-scale contextual information of the encoder-decoder sub-networks is effective for the accurate brain tumor segmentation task. Researchers have presented variant forms of the 3D UNet to extract the enhanced contextual information from MRI [15], [17]. Network’s depth is a common factor to improve the performances among approaches. Residual connection [11] and dense connection [12] are effective to acquire the possible depth in the architecture. Our proposed method used dense connections and the residual inception blocks [24] to extract the meaningful contextual information for brain tumor segmentation. We used densely connected blocks in both encoder-decoder sub-networks to obtain more abstract features. In the previous approach [1], we have used a low number of densely connected blocks as compared to the proposed approach. In the meantime, RIB is used to extract local and global information by merging features of different kernel sizes. In the view of these combinations, our proposed model gives scalable 3D UNet architecture for brain tumor segmentation. The key contributions of this study are given below:

- A novel densely connected 3D encoder-decoder architecture is proposed to extract context features at each level of the network.
- RIB is used to extract local and global information by merging features of different kernel sizes.
- Our network achieves state-of-the-art performance as compared to other recent methods.

2 Proposed Method

Fig. 1 shows our proposed architecture for brain tumor segmentation. In our previous work [1], we have proposed the combined benefits of the residual and dense connections by using *atrous spatial pyramid pooling* (ASPP) [7]. A lack of sufficient contextual information in each block of the encoder-decoder sub-networks limits the performance of the previous model. Moreover, an insufficient number of higher layers can degrade the scores of the model. To address these issues, we designed the novel densely connected 3D encoder-decoder architecture for brain tumor segmentation. In our proposed architecture, we used dense connections to enhance the size of maximum features to 32 in the final output layer. Therefore,

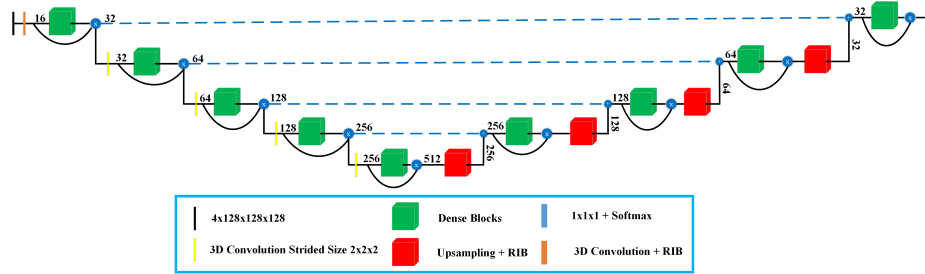


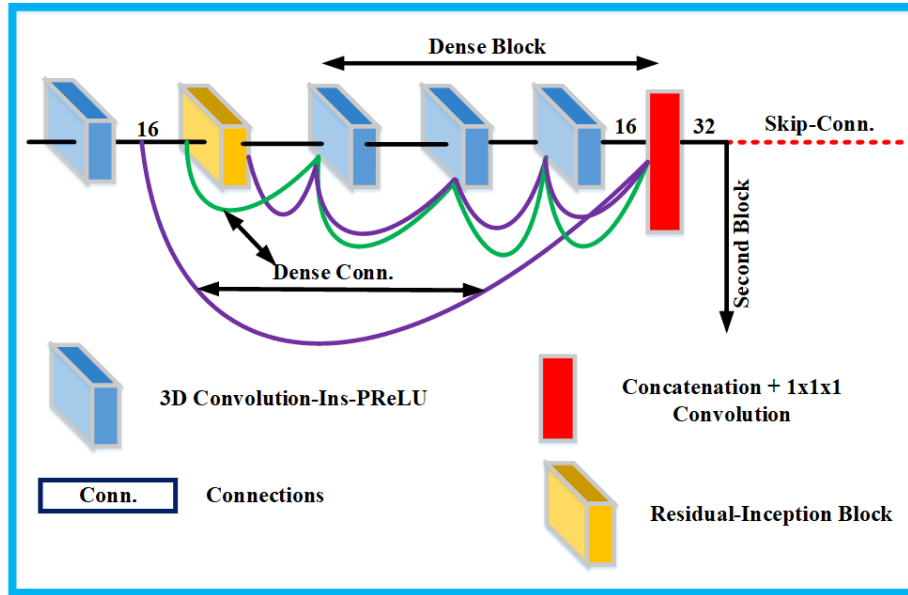
Fig. 1: A densely-connected encoder-decoder 3D architecture for brain tumor segmentation. Each dense block (green) has three weighted layers. The first block of the encoder path has features of RIB to address sizes of tumors. A similar approach is employed after each upsampling process (red) in the decoder part.

the number of features is twice as compared to the previous architecture. The output features at the levels of the encoder path are 32, 64, 128, 256, and 512. Each block of the encoder-decoder paths has three weighted layers except the first block of the encoder path. Fig. 2 exhibits the architecture of the first dense block in the encoder path. RIB is designed with three parallel dilated layers after the first layer in the dense block. The residual connections are mainly employed to prevent the vanishing gradient problem in the deepest models, while the inception blocks provide the required width in the existing residual network. The combined architecture improves the size of the features. These features can further be enhanced with multi-scale strategies [8], [10], [17]. Fig. 3 shows the architecture of the RIB to address the problem of different tumors through multiple sizes of the receptive field. Multi-scale contextual information reduces the number of false positives and prevents the failed segmentation problem. Similar multi-scaled features are employed after each bilinear upsampling layer in the decoder path. Also, the feature size is enhanced more with dense connections before each upsampling layer.

3 Experimental Results

3.1 Dataset

The BRATS aims to bring the research communities together, along with their brilliant ideas for different tasks. Especially for the segmentation task, public benchmark datasets are provided by the organizers. In BRATS 2020, organizers provide 369 subjects for the training, 125 cases for validation, and 166 patients for testing datasets. To train and evaluate our model, we used the BRATS 2020 datasets [2], [3], [4], [5], [20]. In the training dataset, 293 subjects are HGG, while 76 are LGG cases. Four different types of modalities, i.e., $T1$, $T2$, $Flair$, and $T1ce$, are related to each patient in the training, validation, and testing datasets. The training dataset also includes a truth label, i.e., 4, 1, and 2. The



First Dense Block of Encoder Sub-Network

Fig. 2: Proposed densely connected structure in the first block. The first layer and RIB (gold) generate 16 fused maps to the first weighted layer ($3 \times 3 \times 3$ CONV-Instance Normalization-PReLU) in the dense block. In dense block, a dropout rate of 0.2 is employed after the first convolution layer. Moreover, all the preceding maps are the inputs to the next layers, followed by concatenation and non-weighted layer (red) to enhance the size of the output maps (32). Furthermore, the resultant maps are passed to the next dense blocks.

organizers performed necessary pre-processing steps for simplicity. The validation and testing datasets respectively consist of 125 and 166 subjects without ground truth value.

3.2 Implementation Details

We normalize each MRI modality to 0 mean and 1 standard deviation. Our model is built with Keras. We extract patches of size $128 \times 128 \times 128$ from MRI images to feed them into the network. We used five-fold cross-validation, in which each time our network is trained 400 epochs with 16 GB of GPU memory. The batch size is 1, and the initial learning rate is 7×10^{-5} with Adam optimizer. Moreover, we have used regularization techniques to avoid the overfitting problem during the training. We used the dice loss function [21] during the network training. Finally, Table 1 presents the scores of the training, validation, and testing datasets, which are based on the best fold model. We can see the post-processing steps

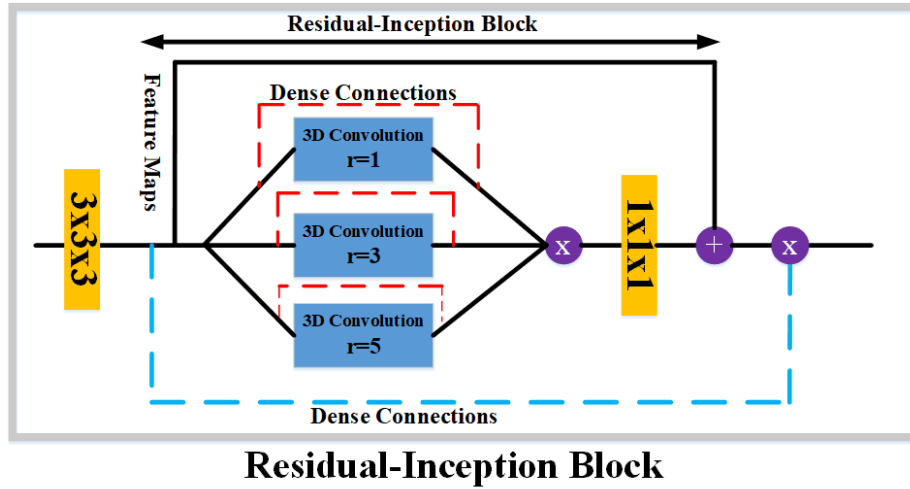


Fig. 3: Proposed RIB structure in the presented approach. The first layer output (gold) is the inputs of the three parallel dilated layers. Output maps of every parallel layer are enhanced with dense connections (dashed red lines) to minimize the problem of multiple sizes of the tumors.

in the future approach. The importance of pre-processing and post-processing algorithms on brain MRI volumes are discussed in the existing works [9], [14], [13].

3.3 Qualitative Analysis

Fig. 4 and Fig. 5 depict the segmentation results of our proposed architecture. Fig. 4 shows the $T1ce$ modality of *HGG* patient from the training dataset, while Fig. 5 depicts the $T1ce$ modalities of two different patients (one from *HGG* and the other from *LGG* datasets). Fig. 4a and Fig. 4c depicted the truth and segmented $T1ce$ modalities while the individual label and prediction are shown in Fig. 4b and Fig. 4d, respectively. Fig. 5a and Fig. 5c shows the segmented $T1ce$ modalities of different patients when RIB is employed in the proposed model, while the segmentation of similar patients without RIB is shown in Fig. 5b and Fig. 5d, respectively. Without RIB, the lack of information in the predicted whole tumor can be observed in Fig. 5b and Fig. 5d, a black arrow denotes the sign lack of information. In contrast, accurate segmentation is presented in Fig. 5a and Fig. 5c.

3.4 Quantitative Analysis

We now evaluate our methods on BRATS datasets of 2018, 2019, and 2020. Table 1 presents the scores of these datasets. Table 2 and Table 3 shows the

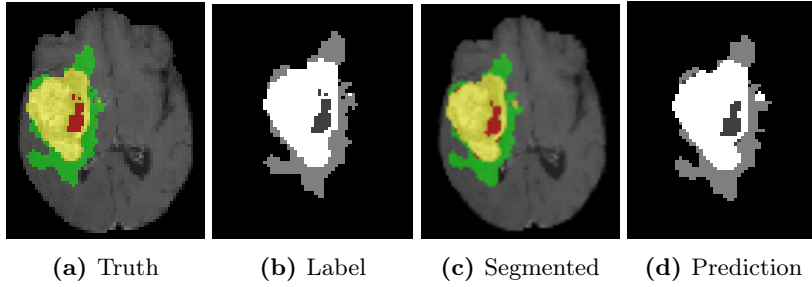


Fig. 4: Segmentation results. (a) and (c) represent the truth and segmented $T1ce$ modalities, while (b) and (d) denote the labeled and predicted modalities, respectively. Different colors represent different tumors: red for TC, green for WT, and yellow for ET.

comparisons between the proposed model and the state-of-the-art methods in the MICCAI BRATS 2018 and 2019 validation datasets, respectively. Table 3 shows the mean DSC value of previous and proposed works. Context-aware 3D UNet approach gains state-of-the-art performances for brain tumor segmentation. We used different dilation rates in the residual inception blocks to address the problem of losing information due to sparsed kernels [25]. The DSC values for WT and TC are best, and ET is lower for both BraTS 2018 and 2019 validation datasets. ET value can be improved by using some post-processing strategies (McKinley [Filtered Output] [19]). Currently, we are studying the influence of dilated and non-dilated convolutional layers on the DSC value of the ET. We will try to improve the mean DSC score of the ET by augmentation techniques based on the classes [26].

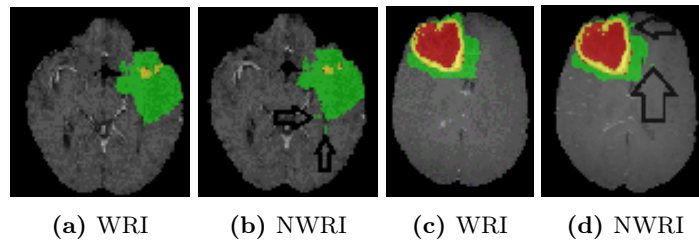


Fig. 5: Segmentation results. (a) and (c) represent the predicted $T1ce$ modalities when RIB is employed in the proposed model (WRI). (b) and (d) represent the predicted $T1ce$ modalities when RIB is removed from the proposed architecture (NWRI).

Table 1: The average scores of different metrics. For BRATS 2018 and 2019, only validation scores are presented. The BRATS organizers validate all the given scores.

Dataset	Metrics	Whole	Core	Enhancing
BRATS 2020 Training	DSC	93.680	91.829	81.677
	Sensitivity	94.052	92.189	82.839
	Specificity	99.934	99.962	99.975
BRATS 2020 Validation	DSC	90.678	84.248	75.635
	Sensitivity	90.390	80.455	75.300
	Specificity	99.929	99.975	99.975
BRATS 2020 Testing	DSC	89.120	84.674	79.100
	Sensitivity	89.983	85.551	84.287
	Specificity	99.929	99.969	99.961
BRATS 2019 Validation	DSC	90.217	83.435	72.289
	Sensitivity	91.570	82.175	79.863
	Specificity	99.370	99.744	99.829
BRATS 2018 Validation	DSC	90.887	85.386	77.270
	Sensitivity	92.171	84.497	84.385
	Specificity	99.464	99.821	99.783

4 Discussion and Conclusion

We have proposed a unique 3D UNet model for brain tumor segmentation. The proposed architecture consists of two sub-modules: (i) dense connections at each level of the encoder-decoder sub-networks, (ii) RIB to extract local and global contextual information by merging feature maps of different kernel’s rate. This

Table 2: Performance evaluation of different methods on the BRATS 2018 validation dataset. For comparison, only DSC scores are shown. All scores are evaluated online.

Methods	Enhancing	Whole	Core
Isensee [baseline] [14]	79.590	90.800	84.320
McKinley [Base + U + BE] [18]	79.600	90.300	84.700
Myronenko [Single Model] [22]	81.450	90.420	85.960
Proposed [Single Model]	77.270	90.887	85.386

Table 3: Performance evaluation of different methods on the BRATS 2019 validation dataset. For comparison, only DSC scores are shown. All scores are evaluated online.

Methods	Enhancing	Whole	Core
Previous Work [ours [1]]	62.301	85.184	75.762
Zhao [BL+warmup+fuse] [15]	73.700	90.800	82.300
McKinley [Raw Output] [19]	75.000	91.000	81.000
McKinley [Filtered Output] [19]	77.000	91.000	81.000
Proposed [Single Model]	72.289	90.217	83.435

study addressed a lack of essential information by using context features at each level of paths. Therefore, the mean average DSC scores of the TC and the WT are improved. In the meantime, the ET score is not improved due to various reasons: (i) zero value of the label ET in *LGG* dataset (we have found 26 and 14 such cases in the BRATS 2020 training and the validation datasets, respectively) (ii) all the presented scores are based on unbiased corrected brain MRI volumes. (iii) the given model has 79 layers, and we are trying to build more depth to address it (iv) our scores are based only on the best fold. However, the literature of the brain tumor segmentation has different useful strategies to improve the final scores, such as the ensembling of different similar models [16], [22] [15], post-processing strategies [14], and pre-processing of brain MRI volumes [9], etc. In the future, we will try to develop light *3D* CNN architectures and investigate the augmentation techniques based on the classes to minimize the class imbalance problem. In summary, our proposed model has the potential to address the problem of other medical imaging tasks.

Acknowledgment

This work is supported by the National Natural Science Foundation of China under Grant No. 91959108.

References

1. Ahmad, P., Qamar, S., Hashemi, S.R., Shen, L.: Hybrid Labels for Brain Tumor Segmentation. In: Crimi, A., Bakas, S. (eds.) *Brainlesion: Glioma, Multiple Sclerosis, Stroke and Traumatic Brain Injuries*. pp. 158–166. Springer International Publishing, Cham (2020)
2. Bakas, S., Akbari, H., Sotiras, A., Bilello, M., Rozycki, M., Kirby, J., Freymann, J., Farahani, K., Davatzikos, C.: Segmentation labels and radiomic features for the pre-operative scans of the TCGA-GBM collection. *The Cancer Imaging Archive* (2017) (2017)
3. Bakas, S., Akbari, H., Sotiras, A., Bilello, M., Rozycki, M., Kirby, J., Freymann, J., Farahani, K., Davatzikos, C.: Segmentation labels and radiomic features for the pre-operative scans of the TCGA-LGG collection. *The Cancer Imaging Archive* **286** (2017)
4. Bakas, S., Akbari, H., Sotiras, A., Bilello, M., Rozycki, M., Kirby, J.S., Freymann, J.B., Farahani, K., Davatzikos, C.: Advancing The Cancer Genome Atlas glioma MRI collections with expert segmentation labels and radiomic features. *Scientific Data* **4**, 170117 (sep 2017), <https://doi.org/10.1038/sdata.2017.117><http://10.0.4.14/sdata.2017.117>
5. Bakas, S., Reyes, M., Jakab, A., Bauer, S., Rempfler, M., Crimi, A., Shinohara, R.T., Berger, C., Ha, S.M., Rozycki, M., Prastawa, M., Alberts, E., Lipková, J., Freymann, J.B., Kirby, J.S., Bilello, M., Fathallah-Shaykh, H.M., Wiest, R., Kirschke, J., Wiestler, B., Colen, R.R., Kotrotsou, A., LaMontagne, P., Marcus, D.S., Milchenko, M., Nazeri, A., Weber, M.A., Mahajan, A., Baid, U., Kwon, D., Agarwal, M., Alam, M., Albiol, A., Albiol, A., Varghese, A., Tuan, T.A., Arbel, T., Avery, A., B., P., Banerjee, S., Batchelder, T., Batmanghelich,

- K.N., Battistella, E., Bendszus, M., Benson, E., Bernal, J., Biros, G., Cabezas, M., Chandra, S., Chang, Y.J., al., E.: Identifying the Best Machine Learning Algorithms for Brain Tumor Segmentation, Progression Assessment, and Overall Survival Prediction in the {BRATS} Challenge. CoRR **abs/1811.02629** (2018), <http://arxiv.org/abs/1811.02629>
6. Chen, L., Bentley, P., Mori, K., Misawa, K., Fujiwara, M., Rueckert, D.: DRINet for Medical Image Segmentation. *IEEE Transactions on Medical Imaging* **37**(11), 2453–2462 (nov 2018). <https://doi.org/10.1109/TMI.2018.2835303>
 7. Chen, L.C., Papandreou, G., Schroff, F., Adam, H.: Rethinking Atrous Convolution for Semantic Image Segmentation. CoRR **abs/1706.0** (2017), <http://arxiv.org/abs/1706.05587>
 8. Dolz, J., Gopinath, K., Yuan, J., Lombaert, H., Desrosiers, C., Ayed, I.B.: HyperDense-Net: A hyper-densely connected CNN for multi-modal image segmentation. CoRR **abs/1804.0** (2018), <http://arxiv.org/abs/1804.02967>
 9. Feng, X., Tustison, N., Meyer, C.: Brain Tumor Segmentation Using an Ensemble of 3D U-Nets and Overall Survival Prediction Using Radiomic Features. In: Crimi, A., Bakas, S., Kuijff, H., Keyvan, F., Reyes, M., van Walsum, T. (eds.) *Brainlesion: Glioma, Multiple Sclerosis, Stroke and Traumatic Brain Injuries*. pp. 279–288. Springer International Publishing, Cham (2019)
 10. Havaei, M., Davy, A., Warde-Farley, D., Biard, A., Courville, A.C., Bengio, Y., Pal, C., Jodoin, P.M., Larochelle, H.: Brain Tumor Segmentation with Deep Neural Networks. CoRR **abs/1505.0** (2015), <http://arxiv.org/abs/1505.03540>
 11. He, K., Zhang, X., Ren, S., Sun, J.: Deep Residual Learning for Image Recognition. CoRR **abs/1512.0** (2015), <http://arxiv.org/abs/1512.03385>
 12. Huang, G., Liu, Z., Weinberger, K.Q.: Densely Connected Convolutional Networks. CoRR **abs/1608.0** (2016), <http://arxiv.org/abs/1608.06993>
 13. Isensee, F., Kickingereder, P., Wick, W., Bendszus, M., Maier-Hein, K.H.: Brain Tumor Segmentation and Radiomics Survival Prediction: Contribution to the {BRATS} 2017 Challenge. CoRR **abs/1802.1** (2018), <http://arxiv.org/abs/1802.10508>
 14. Isensee, F., Kickingereder, P., Wick, W., Bendszus, M., Maier-Hein, K.H.: No New-Net. In: Crimi, A., Bakas, S., Kuijff, H., Keyvan, F., Reyes, M., van Walsum, T. (eds.) *Brainlesion: Glioma, Multiple Sclerosis, Stroke and Traumatic Brain Injuries*. pp. 234–244. Springer International Publishing (2019)
 15. Jiang, Z., Ding, C., Liu, M., Tao, D.: Two-Stage Cascaded U-Net: 1st Place Solution to BraTS Challenge 2019 Segmentation Task. In: Crimi, A., Bakas, S. (eds.) *Brainlesion: Glioma, Multiple Sclerosis, Stroke and Traumatic Brain Injuries*. pp. 231–241. Springer International Publishing, Cham (2020)
 16. Kamnitsas, K., Bai, W., Ferrante, E., McDonagh, S.G., Sinclair, M., Pawlowski, N., Rajchl, M., Lee, M.C.H., Kainz, B., Rueckert, D., Glocker, B.: Ensembles of Multiple Models and Architectures for Robust Brain Tumour Segmentation. CoRR **abs/1711.0** (2017), <http://arxiv.org/abs/1711.01468>
 17. Kamnitsas, K., Ledig, C., Newcombe, V.F.J., Simpson, J.P., Kane, A.D., Menon, D.K., Rueckert, D., Glocker, B.: Efficient multi-scale 3D CNN with fully connected CRF for accurate brain lesion segmentation. *Medical image analysis* **36**, 61–78 (2017)
 18. McKinley, R., Meier, R., Wiest, R.: Ensembles of Densely-Connected CNNs with Label-Uncertainty for Brain Tumor Segmentation. In: Crimi, A., Bakas, S., Kuijff, H., Keyvan, F., Reyes, M., van Walsum, T. (eds.) *Brainlesion: Glioma, Multiple Sclerosis, Stroke and Traumatic Brain Injuries*. pp. 456–465. Springer International Publishing, Cham (2019)

19. McKinley, R., Rebsamen, M., Meier, R., Wiest, R.: Triplanar Ensemble of 3D-to-2D CNNs with Label-Uncertainty for Brain Tumor Segmentation. In: Crimi, A., Bakas, S. (eds.) *Brainlesion: Glioma, Multiple Sclerosis, Stroke and Traumatic Brain Injuries*. pp. 379–387. Springer International Publishing, Cham (2020)
20. Menze, B.H., Jakab, A., Bauer, S., Kalpathy-Cramer, J., Farahani, K., Kirby, J., Burren, Y., Porz, N., Slotboom, J., Wiest, R., Lanczi, L., Gerstner, E., Weber, M., Arbel, T., Avants, B.B., Ayache, N., Buendia, P., Collins, D.L., Criminisi, A.: The Multimodal Brain Tumor Image Segmentation Benchmark (BRATS). *IEEE Transactions on Medical Imaging* **34**(10), 1993–2024 (oct 2015). <https://doi.org/10.1109/TMI.2014.2377694>
21. Milletari, F., Navab, N., Ahmadi, S.A.: V-Net: Fully Convolutional Neural Networks for Volumetric Medical Image Segmentation. *CoRR* **abs/1606.0** (2016), <http://arxiv.org/abs/1606.04797>
22. Myronenko, A.: 3D {MRI} brain tumor segmentation using autoencoder regularization. *CoRR* **abs/1810.1** (2018), <http://arxiv.org/abs/1810.11654>
23. Ronneberger, O., Fischer, P., Brox, T.: U-Net: Convolutional Networks for Biomedical Image Segmentation. *CoRR* **abs/1505.0** (2015), <http://arxiv.org/abs/1505.04597>
24. Szegedy, C., Ioffe, S., Vanhoucke, V.: Inception-v4, Inception-ResNet and the Impact of Residual Connections on Learning. *CoRR* **abs/1602.0** (2016), <http://arxiv.org/abs/1602.07261>
25. Wang, P., Chen, P., Yuan, Y., Liu, D., Huang, Z., Hou, X., Cottrell, G.W.: Understanding Convolution for Semantic Segmentation. *CoRR* **abs/1702.0** (2017), <http://arxiv.org/abs/1702.08502>
26. Wang, Q., Gao, J., Yuan, Y.: A Joint Convolutional Neural Networks and Context Transfer for Street Scenes Labeling. *IEEE Transactions on Intelligent Transportation Systems* **19**(5), 1457–1470 (may 2018). <https://doi.org/10.1109/TITS.2017.2726546>